

Review of the PV Electricity Production Estimate under the Effect of Climatic Disturbances and Sunspots by Using Deep-Learning Tools

Afef Ben Othman^{1,2}, Ayoub El Ouni^{1,3} and Mongi Besbes^{1,4,*}

¹Laboratory of Robotics, Informatics and Complex System, University of Tunis El Manar, Tunis, Tunisia; ²National School of Engineers of Carthage, University of Carthage, Carthage, Tunisia; ³Higher Institute of Environmental Sciences and Technologies, University of Carthage, Carthage, Tunisia and ⁴Higher Institute of Information and Communication Technologies, University of Carthage, Carthage, Tunisia

Abstract: The mathematical models used in the estimation of GHI on the Earth's surface are inconvenient because they always assume that the sky clarity index is constant. Hence, these models are often confronted with long-period empirical ground measurements that may exceeds 11 years. The impact of cloud cover on an electric power generation site is a very critical parameter for installing a solar power plant and evaluating its productivity. The state of knowledge about the sun influence, the greenhouse effect on climate change, and cloud occurrence can't be described in a mathematical or numerical model.

Therefore, in this paper, we propose the use of Deep-Learning techniques to predict any site's productivity by analyzing its potential insolation. We also suggest the analysis of the ground and satellite-based measurements collected over 30 years. We propose the estimation of future climate change affecting cloud cover.

Keywords: Photovoltaic and solar thermal energy, sunspots, greenhouse effect, climate change, numerical modeling, Deep-Learning, GHI Prediction.

1. INTRODUCTION

The photovoltaic or thermodynamic electrical energy productivity of a geographic site is strongly related to the amount of solar irradiation to which it is exposed. This amount of irradiation does not depend on the solar activity and the geographical coordinates of the place but also the area's cloud cover during the year [1-5].

The use of mathematical models to estimate the site's production of energy assumes that the clarity index is constant and therefore does not consider climatic conditions [6, 7]. The vast majority of climate scientists agree that the earth is now facing global climate change, which affects local climate more than ever before. Although there has been consensus that climate change is a human-based disturbance influenced by human activities such as the greenhouse effect, climatologists have recently stated that the phenomenon can have correlation with the solar activity and the possible effects of sunspots. For other researchers, these correlations are unclear and require much more evidence.

The first research on the issue dates back to more than two centuries when the English astronomer William Herschel argued for a systematic correspondence

between solar activity and the climate change. Countless works have since been published on this subject, which remains controversial for several major reasons:

- the detected correlations did not continue over time.
- the authors did not consider the superposition of other forcing over the same time scales or uncertainties.
- the systematic bias in the used climate data, or even misuse of the statistical tools.

However, evidence of the link between solar activity and climate change at different time scales and several compartments of the climate system has continued to accumulate. A classic example is the influence of the 11-year cycle on stratospheric temperatures and wind. The impact of this cycle on the dynamics of the troposphere has also been the subject of several studies, notably on possible systematic variations of the geometry and the intensity of the large-scale average circulation (e.g., Hadley cells, jet streams, and Walker circulation).

The empirical studies on the sun-climate link have also been conducted for even longer time scales, including the relationship between the "Great Minima" of solar activity and the Little Ice Age. Much progress has been achieved thereafter through the reconstruction of climatic conditions dating back to the last

*Address correspondence to this author at the Laboratory of Robotics, Informatics and Complex System, University of Tunis El Manar, Tunis, Tunisia; Tel: +216 98 819 453; E-mail: mongi.besbes@gmail.com; mongi.besbes@istic.u-carthage.tn

millennia across different geographical areas and different climate system compartments. Research progress has also been reached through the study of solar activity on the same time scales from cosmogenic nuclides ^{10}Be and ^{14}C .

Comparative data analysis was also significant for research progress because it does not only allow highlighting the solar activity impacts, but also the identification of complications. This analysis has revealed that solar forcing is combined with several natural external forcings causing climate change and occurring on the same time scales. In addition, paleoclimatic records show spatial heterogeneity suggesting the importance of regional processes. It should thus be emphasized that the evocative terms Little Ice Age and Medieval Optimum simplify contrasting realities with significant temporal and spatial variability.

The evaluation of the solar component in the climate series necessarily involves a multivariate statistical analysis taking into account the additional natural external forcing factors such as volcanic eruptions, greenhouse gases, and the oscillations intrinsic to the climate system (e.g., ENSO variability, El-Nino, and Southern Oscillation). Indeed, solar forcing, dominated by the 11-year cycle, does not show a long-term increase; considering the precise measurements of irradiance over 30 years and the modulation cosmic rays. This suggests the likely influence of other forcing factors, including that of greenhouse gases whose

concentrations have risen continuously over the same period (see Figure 1).

The temporal correlation between the solar forcing and climate change is not enough to establish a causal link; therefore, to consider a second path based on mechanisms and associated climate feedbacks is imperative.

Several works have studied in detail the hypothesis of the existence of an impact of cosmic rays on the formation of condensation nuclei and their consequences on the atmosphere. These studies have been conducted based on ground and aerial observations of the atmospheric aerosol formation, the case of rapid perturbations of galactic cosmic radiation during Forbush effects associated with coronal mass ejections from the Sun, and the first numerical simulations integrating the formation of condensation nuclei by cosmic radiation. These recent works, different and complementary in their approaches, lead for the moment to the conclusion that cosmic rays do not have major influence on the current climate.

Research on climate change still entails many uncertainties and recent works will have to be reproduced and verified. Moreover, it would be wise to wait for the conclusions of the experimental approach conducted at CERN, even if the preliminary results underline the difficulties of the CLOUD experiment. Furthermore, other hypotheses of interaction between the ionizing

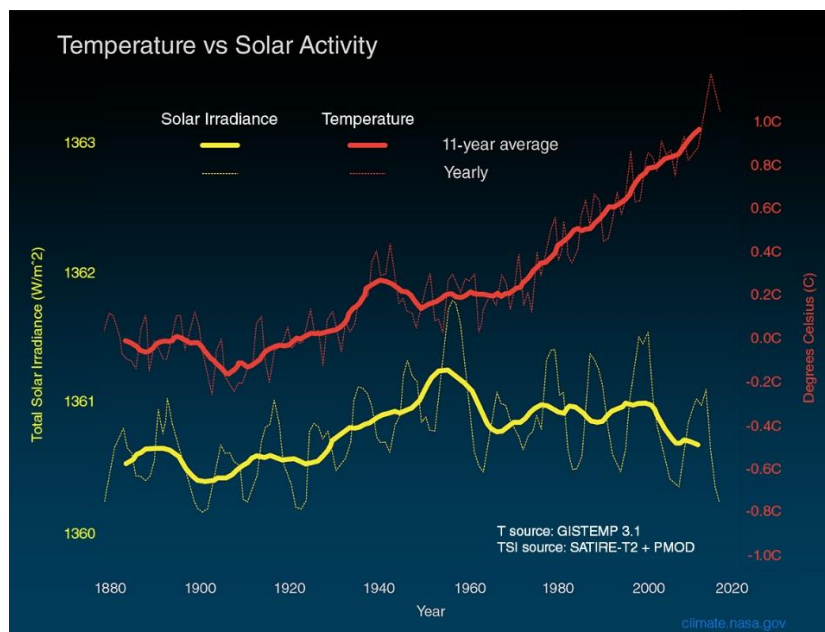


Figure 1: Solar activities over years. (© NASA, Global Climate Change).

particles and the atmosphere have been envisaged and will have to be the subject of direct observations and numerical modeling. Similarly, observations and models in solar astrophysics should tell us much more about the modes of variation of the Sun at different time scales. All these mechanisms deserve further study; the importance of their role needs to be established on a convincing scientific basis.

This paper is divided into 4 parts.

In the first part, we discuss the effect of the solar cycle and the appearance of tasks on the climate. The analysis will focus on the results of recent research. We provide an overview the persistent debate among the scholarly community over the drivers of climate change. Some claim that the ultraviolet that accompanies the sunspots is responsible for raising the temperature. Conversely, critics of this view tend to minimize the effect of the Sunspots and attribute the increase in temperature to the greenhouse impact and human activities.

In the second part, we present the use of Machine Learning's new techniques, in this case Deep Learning, as a more effective alternative for the prediction of the evolution of solar sunstrokes during the next 10 years. This part focuses on the combined effectiveness of deep neural networks and advances in artificial intelligence.

The third part is devoted to a case study, where the cogency of the neural networks is used to predict the quantity of future GHI on the photovoltaic and thermo-solar production zone in southern Tunisia. Our investigation is based on measurements of temperature, wind, solar insolation, GHI and solar spots, over 30 years of ground measurements and satellite imagery from NASA. We use this collected data to predict whether there exists any changes in production in the selected site and if there are any special measures to be taken.

The paper ends with a conclusion tracing the possible contributions of this work and the possible prospects.

2. SOLAR ACTIVITY AND CLIMATE CHANGE

2.1. Solar Activity

Solar radiation is the main source of heat on Earth. But the Sun is a rather special star. It is one of the few stars whose brightness, size and explosions are relatively constant. The brightness of the star only

varies by 0.1% over an 11-year cycle. However, even this small variation can have a significant effect on the Earth's climate.

The Sunspots appear in the photosphere as a dark area (the shadow) surrounded by a lighter region (the penumbra), are colder than the ambient photosphere (4,500 K against about 5,800 K for the photosphere), and are due at cooling following the inhibition of surface convection by the local increase of the magnetic field. Their largest dimension can reach tens of thousands of km [8].

The spots often appear in groups and are often accompanied by other spots of opposite magnetic polarity (group of bipolar spots). At the beginning of the solar cycle, the spots appear preferably at high latitude in both hemispheres (around 40°). Generally, the first spots of a group are of the same polarity [9]. Throughout the cycle, the spots will move closer to the equator until the beginning of the next cycle. At this point, the polarity of the spots must change.

From the Earth, the influence of the sun varies mainly according to a daily and annual period. In absolute terms, the activity is regulated by a solar cycle with an average period of 11.2 years - from one maximum to the next - but the duration can vary between 8 and 15 years. The amplitude of the maxima can vary from simple to triple.

During years of peak activity, there is an increase in the:

- number of sunspots and solar bursts;
- corpuscular radiation;
- electromagnetic radiation.

Sunspots reveal the convection of the solar plasma. This ionized material forms convection cells, and the plasma flows dip at the equator and rise at the poles. With an average speed of 65 km/h, these plasma flows take eleven years to complete the convection cell and be at the origin of the solar cycle. This solar cycle results in a strong modulation of the number of visible sunspots. In addition, there is a longer-scale modulation of solar activity by its spots. The maximum number of sunspots visible at the maximum of the solar cycle varies over time and is correlated with the variation of solar magnetic fields [10].

Sunspots are darker and colder than the sun's surface and therefore decrease the intensity of solar

radiation. But they are accompanied by bright spots that increase the intensity of solar radiation. It is the effect of light spots that prevails so that the solar radiation is higher; reaching about 0.1% during periods of high solar activity. This difference may seem small but represents a significant difference in the energy received for a system like Earth. Thus, the heart of the Little Ice Age, covering the period 1550-1850 was thus marked by a very low number of sunspots, or even their complete disappearance in around 1665-1700.

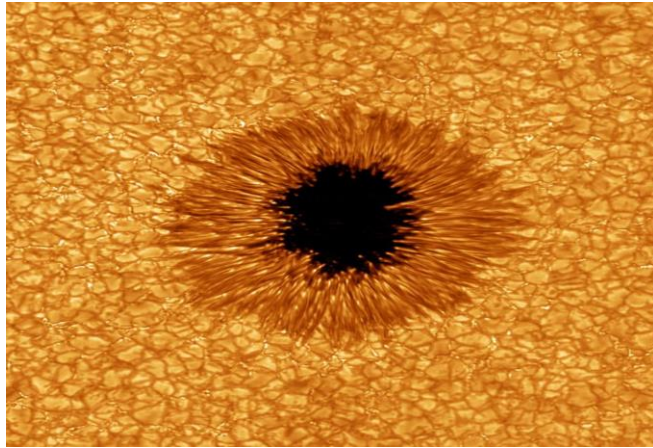


Figure 2: *A photographic image of a Sunspot.* (© Big Bear Solar Observatory).

A sunspot is a dark area that appears intermittently on the apparent surface of the sun. The greater is the activity of the sun, the more sunspots will appear (Figure 2). This sunspot image obtained using the New Solar Telescope has an exceptional resolution. Each of these grains is approximately 1,000 kilometers long and the smallest details are close to 65 kilometers. (© Big Bear Solar Observatory.)

Researcher Greg Kopp of the University of Colorado's Atmospheric Physics and Space Laboratory explains that even an increase in incident solar radiation of 0.1% is important. It provides more energy than all other sources combined (the natural radioactivity of the Earth's core for example) [11].

The 0.1% characterizes the global spectrum of the sun, all the wavelengths. But during solar activity peaks, the star emits ultraviolet (UV) radiation ten times more than average. Emissions in this spectral band can strongly affect the chemistry and temperature of the atmosphere.

The stratospheric ozone layer protects Earth's surface from ultraviolet radiation, which is dangerous

for any living being on the planet. The energetic particles of Sun create nitrogen oxides emitted during peaks of solar activity, and which can reduce the ozone rates. Thus, when the sun goes through a peak of activity, more UV rays reach the surface of the earth and warm the atmosphere [12].

It is difficult to accurately quantify the impact of solar activity because all the scientific disciplines must be interacted and applied to multiple layers of the atmosphere. Some researchers rely on chemistry, others on thermodynamics and others on fluid mechanics. The problem is therefore complex, but that does not mean that it is not real [13].

For example, the National Center for Atmospheric Research (NCAR, USA) provided, in a 2012 report, some compelling evidence of the impact of solar variability on the climate. During a peak of solar activity, a configuration like the La Niña phase of the El Niño cycle takes shape in the Pacific. There is a cooling of nearly 1 °C in the eastern equatorial Pacific. In addition, increased precipitation has been observed in the Inter-Tropical Convergence Zone (ITCZ) and the South Pacific Convergence Zone (SPCZ). Solar cycle signals are so strong in the Pacific that some wonder about what amplifies the signals of solar activity in the region.

The question of the role of the solar cycle in global warming has already been debated. The sun is the main source of heat. So it would not be so preposterous to imagine that variations in its activity play a role in global warming. Many have pointed out that before the Little Ice Age, solar activity was minimal for 70 years (this is Maunder's minimum). But the NRC report says that the influence of the sun is certainly noticeable, but on a regional rather than global scale [14].

When the radiative balance of the Earth is altered, as in the case of a change in the solar forcing cycle, all the regions does not get equally affected. According to NCAR researchers [15] the central Equatorial Pacific is generally colder, the flow of rivers in Peru is reduced, and drier conditions are affecting the western United States.

In addition, the report states that the effect of solar energy changes is manifested in alterations in the general atmospheric circulation rather than in straight changes in temperature degrees. These statements are consistent with the findings of the GIEC latest report and previous CNRC reports. According to all

these scientific organizations, solar variability is not the cause of the warming that the planet has known for more than 50 years.

2.2. The Effects on the Climate

In order to quantify the impact of human activity on the climatic variations observed in recent years, it is necessary to evaluate the contribution of natural forcing. In the present context, however, the exact contributions of each forcing (i.e. anthropogenic or natural) are still subject to discussion. This determination is also a major issue for future predictions of climate change. It is therefore important to quantify the contributions of natural forcing, and solar forcing, which is the main component of this natural climate variability. Recent estimates from the 5th report of the IPCC (2013) show that solar radiative forcing contributed 0.05 Wm^{-2} to global warming between 1750 (industrial pre-revolution period) and 2011. This contribution is given with an uncertainty of between 0.00 and 0.10 Wm^{-2} . It is significantly lower than that estimated for radiative forcing of anthropogenic origin, over the same period, whose contribution amounts to 2.29 Wm^{-2} (with a range between 1.13 and 3.33 Wm^{-2}).

These results also suggest that radiative changes of solar origin played a major role until the beginning of the second half of the 20th century (1950). From this date on, radiative forcing from the original greenhouse gases anthropic became dominant. The impact of solar variability on the climate is quite complex. Indeed, this variability influences the climate according to different mechanisms but also at different time scales. These different mechanisms are classified according to their effects on the climate direct and indirect effects. The direct effect is purely radiative and results in the variation of solar energy reaching the Earth system (atmosphere + ocean).

Other effects on climate are indirect. The most important of these effects is the effect of solar variability on the stratosphere and more particularly on stratospheric ozone. Indeed, ozone is the key radiative gas of the stratosphere, so it plays a key role in the radiative balance of the atmosphere. The study of the various processes causing global warming has progressed with the multiplication of observations and calculation methods. Since the advent of the space age (late 70s), many satellite data have become available. Recent satellite measurements of solar UV variability have shown some consensus [16]. This variability is also well reproduced by ultraviolet flux reconstruction models [17-20].

However, this situation evolved following the launch of the SIM instrument aboard the *SORCE* satellite in 2003. Indeed, the measurements of the solar flux by the SIM / *SORCE* instrument showed totally unexpected results. The data measured by SIM / *SORCE* show a 4- to 6-fold decrease in the UV range (200-400 nm) between 2004 and 2008 [21]. This sharp decrease is compensated by an increase in the visible range so that the variability of total solar irradiance (integrated solar flux at all wavelengths) remains equivalent to that described by the other satellites and reconstruction models between the minimum and maximum of an 11-year solar cycle (i.e., 0.1%).

When solar forcing from SIM / *SORCE* data is used in climate-chemistry models, the response of the Earth system is very different from that of solar forcing from a commonly used reconstruction model (NRL-SSI model, [22]). For example, heating rates (SW) are much higher in the upper stratosphere. In addition, the ozone response over the period 2004-2007 appears positive in the lower stratosphere and negative over 45 km while that obtained from reconstructed forcing has positive values over the entire vertical domain. These radiative and photochemical differences can strongly modify our understanding of the impact of solar variability on the stratosphere but also on the climate. Moreover, forced model results from the solar spectra of SIM / *SORCE* appear to be in better agreement with some satellite data sets than the results from solar spectrum reconstruction models [23, 24].

Nevertheless, the SIM / *SORCE* measures remain tainted by statistical and instrumental uncertainties. This would tend to nuance the previous results, as evidenced by the study made by Merkel *et al.* [24] in which possible errors of calibration of the instrument could be the cause of a two-fold overestimation of the variability solar flux in the UV range. In addition, the MIS data used in these studies do not cover a complete solar cycle and it is therefore necessary to extrapolate them, which has resulted in added uncertainty [25]. Beyond these uncertainties, SIM data could challenge our understanding of the different stratospheric processes induced by solar variability. The debate around ozone data SIM / *SORCE* remains open pending new data and studies.

Since the late 1990s, Danish researchers have announced that they have identified the 11-year cycle in satellite cloud cover records. These works have focused on several types of clouds according to their altitudes. Nevertheless, the correspondences ann-

ounced have not been confirmed by the most recent studies. The basic processes are governed by physicochemical laws and the assessment of their influence on the global and regional climate can be carried out using numerical models of climate.

The variety of forcing implies that these models have a high level of sophistication while allowing long simulations of several centuries. The use of general circulation models makes it possible to finely study the climatic feedbacks that amplify or attenuate the radiative signal related to a forcing as well as to consider the multiple combination of forcing.

It must be emphasized that the climatic impact of clouds strongly depends on their radiative properties and therefore on their altitude. The solar modulation planned in 1997 was expected to induce a decrease in high altitude clouds at high latitudes during a period of high solar activity. However, these high-altitude clouds generally tend to heat the Earth's surface, and not to cool it as low-altitude clouds do. The hypothesis was therefore incompatible with the apparent correlation between solar activity and warming during the second part of the twentieth century. These authors then modified their analysis by proposing a solar influence limited to the low altitude clouds whose cover seemed to better follow the solar fluctuations. This change of hypothesis may be surprising because one would rather expect a maximum solar effect for the upper part of the atmosphere and not for its lowest part in which the condensation nuclei already abound.

The interaction between solar radiation and Earth is complex because it involves many scientific disciplines. To understand how solar energy affects the climate, one must consider plasma physics, atmospheric chemistry, fluid mechanics, and particle physics. It is necessary to carry out an assessment of the expertise of different teams which make it possible to frame the problem.

3. DEEP LEARNING

Overall, the goal of deep learning is to solve "intuitive" problems they are characterized by a strong dimensionality and the absence of rules [26]. The use of deep learning is best suited for situations involving large amounts of data and complex relationships between different parameters. Training a neural network consists of repeatedly showing that "Given the input, the output is the right one". If this is done enough times, a network will mimic the function that one wishes

to simulate. He will also ignore any entries that are irrelevant to the solution. Conversely, it will fail to converge to a solution if it does not receive critical inputs. For this reason Deep-Learning applies to many fields [27].

It is now possible to implement deep learning for three reasons: the high power of CPU / GPUs, powerful algorithms and the existence of data sets. Over the next few years, these factors will lead to other applications. They are best suited for situations that involve large amounts of data and complex relationships between different parameters.

Solve an intuitive problem: to form a network of neurons requires to demonstrate repeatedly that: "Given the input, this is the correct output". If this is done often enough, a network will mimic the function we want to simulate [28].

An artificial neuron will receive electrical signals. When it receives enough signals to send itself, it will send electrical signals to another artificial neuron are formed. Thus, when creating an end-to-end technology made of a multitude of neurons, then networks of neurons are formed. This technology makes it possible to solve problems that are too complex for the human brain, in an infinitely reduced time because the transmission of information from one neuron to another is counted in a few milliseconds [29].

The perceptron is a single layer neuron network invented by Rosenblatt. Figure (3) shows that it is formed by a first layer of units (or neurons) that make it possible to "read" the data. Each unit corresponds to one of the input variables. We can add a bias unit that

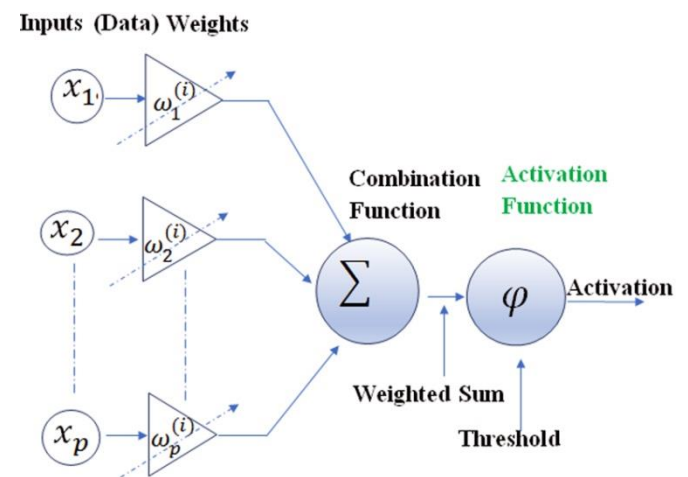


Figure 3: Scheme of a perceptron.

is always activated (it transmits 1 regardless of the data). These units are connected to a single output unit, which receives the sum of the units connected to it, weighted by connection weights [30].

For P variables x_1, x_2, \dots, x_p the output therefore receives:

$$\omega_0 + \sum_{j=1}^p \omega_j x_j \quad (1)$$

The output unit then applies an activation function a to this output.

A perceptron predicts therefore thanks to a decision function f which is given below:

$$f(x) = a \left(\omega_0 + \sum_{j=1}^p \omega_j x_j \right) \quad (2)$$

This function has an explicit form, it is a parametric model.

In the case of a regression problem, it is not necessary to transform the weighted sum received into input. The activation function is the identity function; it fully returns what it has received.

In the case of a binary classification problem, one can use a threshold function:

$$s \left(\omega_0 + \sum_{j=1}^p \omega_j x_j \right) = \begin{cases} 0 & \text{if } a \left(\omega_0 + \sum_{j=1}^p \omega_j x_j \right) < 0 \\ 1 & \text{if not} \end{cases} \quad (3)$$

As in the case of logistic regression, we can also use a sigmoid function to predict the probability of belonging to the positive class:

$$\sigma \left(\omega_0 + \sum_{j=1}^p \omega_j x_j \right) = \frac{1}{1 + e^{-\left(\omega_0 + \sum_{j=1}^p \omega_j x_j \right)}} \quad (4)$$

In the case of a multi-class classification problem, we will modify the architecture of the perceptron. Instead of using a single output unit, it will use as many classes as possible. Each of these units will be connected to all input units. We thus have $K(p + 1)$ connection weight, where K is the number of classes.

The *softmax* function can then be used as an activation function. This is a generalization of the sigmoid, which can also be written as:

$$\sigma(u) = \frac{1}{1 + e^u} \quad (5)$$

We are going to use:

$$\sigma_k(u_k) = \frac{e^{u_k}}{\sum_{j=1}^k e^{u_j}} \quad (6)$$

If the output for the class k is sufficiently larger than those of the other classes, its activation will be close to 1 while the activation of the others will be close to 0. We can also consider that it is a version differentiated from the maximum, which will greatly help us for learning (Figure 4).

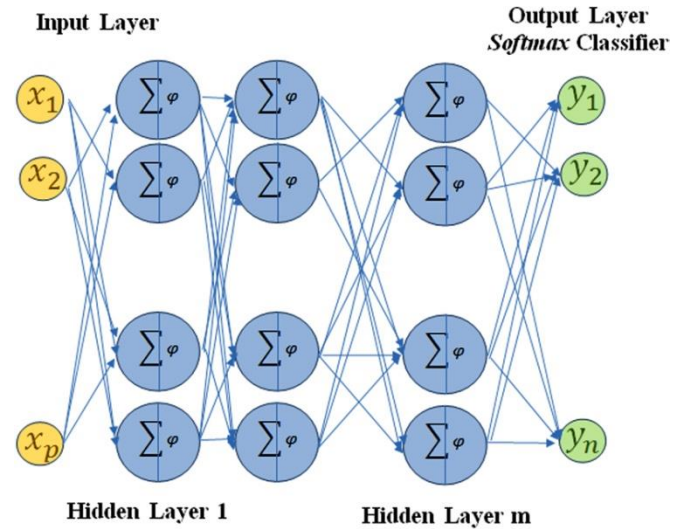


Figure 4: Neuron Network for Deep-Learning.

3.1. Training of one Perceptron

To train a perceptron, i.e., to learn the connection weights, we will try to minimize the prediction error on the training game. We could do this explicitly, as in the case of the least square's method for linear regression. However, this is not probably how a network of biological neurons works [31].

Moreover, biological neural networks are supposed to be plastic beings. That is to say they adapt constantly, according to the signals they receive. Thus, we will assume that our n observations $x^{(1)}, x^{(2)}, \dots, x^{(n)}$ are not observed simultaneously but sequentially, one after the other.

Thus, neural networks are driven by so-called incremental or online learning algorithms, as opposed to the models we have seen so far, which are driven by offline algorithms (batch learning). An intermediate solution is to consider that the observations arrive small packet by small packet, so-called mini-batch learning.

The training of a perceptron is therefore an iterative process. After each observation, we will adjust the connection weights to reduce the prediction error made by the perceptron in its current state. For that reason, we will use the algorithm of the gradient. With the gradient giving us the direction of greater variation of a function (in our case, the function of error), to find the minimum of this function it is necessary to move in the opposite direction to the gradient. (When the function is locally minimized, its gradient is 0) [32].

Thus, we start by randomly choosing initial values $\omega_0^{(0)}, \omega_1^{(0)}, \dots, \omega_p^{(0)}$ for our connection weights. Then, after each observation $(x^{(i)}, y^{(i)})$, we will apply to each weight the following update rule:

$$\omega_j^{(t+1)} = \omega_j^{(t)} - \eta \frac{\partial \varepsilon(f(x^{(i)}), y^i)}{\partial \omega_j} \quad (7)$$

You can iterate several times over the entire dataset. It is usually iterated until the algorithm converges (the gradient is close enough to 0) or, more frequently, for a fixed number of iterations (Figure 5).

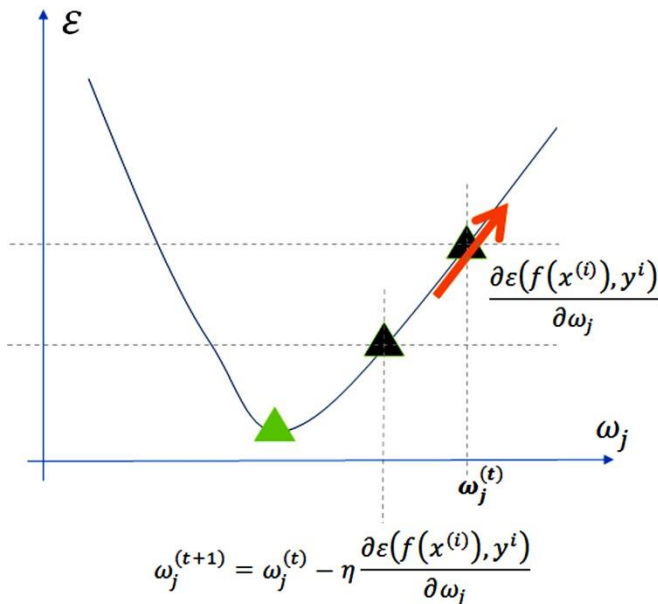


Figure 5: Gradient algorithm convergence.

η is a hyperparameter of the neural network, called the learning rate.

If η is large, we move far away from $\omega_j^{(t)}$. If this point is already close to the optimal value, we risk exceeding our objective and $\omega_j^{(t+1)}$ is further than $\omega_j^{(t)}$ from its optimal value. The algorithm is likely to diverge, that is, to move away from the optimal solution [33].

On the other hand, if $\omega_j^{(t)}$ is far from its optimal value and η is weak, the algorithm will take a very long time to converge.

It is therefore important to choose the speed of learning. There are algorithms to adapt this speed so that it is raised far from the solution and weaker in its vicinity.

3.2. Defining the Error Function

In the case of regression, we will choose the quadratic error (as for a linear regression):

$$\varepsilon(f(x^{(i)}), y^{(i)}) = \frac{1}{2} (y^{(i)} - f(x^{(i)}))^2 = \frac{1}{2} \left(y^{(i)} - \sum_{j=1}^p \omega_j x_j^{(i)} \right)^2 \quad (8)$$

The update rule is therefore:

$$\omega_j^{(t+1)} = \omega_j^{(t)} - \eta (y^{(i)} - f(x^{(i)})) x_j^{(i)} \quad (9)$$

In the case of classification, we will choose cross entropy. In the binary case the cross entropy is defined by:

$$\varepsilon(f(x^{(i)}), y^{(i)}) = -y^{(i)} \log(f(x^{(i)})) - (1 - y^{(i)}) \log(1 - f(x^{(i)})) \quad (10)$$

Cross entropy is a little more complicated to differentiate than squared error. But after few calculations it turns out that the rule of updating connection weights is the same as that of the quadratic one.

And this is also true for the multiclass version of cross entropy:

$$\varepsilon(f(x^{(i)}), y^{(i)}) = - \sum_{k=1}^K y_k^{(i)} \log(f_k(x^{(i)})) \quad (11)$$

the updated rule is:

$$\omega_j^{(t+1)} = \omega_j^{k(t)} - \eta (y^{(i)} - f_k(x^{(i)})) x_j^{(i)} \quad (12)$$

The perceptron allows to learn parametric models based on a linear combination of variables.

- The perceptron allows to learn regression models (the activation function is the identity), binary classification (the activation function is the logistic function) or multi-class classification (the activation function is the *Softmax* function).
- The perceptron is driven by iterative updates of its weights through the gradient algorithm. The

same rule for updating weights applies in the case of regression, binary classification or multi-class classification.

Thus, all the neurons interact with each other, forming dozens of "layers" of data and calculations. This is why we call this process "deep learning". Each of the neurons performs calculations, which will be communicated to the layers, which will themselves communicate between layers and validate or invalidate the results they expected according to the information transmitted by the artificial neurons. This will allow the AI to achieve the mission for which it is created [34]

At each level of artificial neurons, there can be multiple layers. Thanks to the interactions between the artificial neurons, the AI will, as and when, deepen its knowledge in a given field. It becomes an expert because it can consider all the parameters necessary for its understanding of the environment it is studying [35]. Deep Learning is in a process of self-learning. As it gains access to thousands of data, it will be able to learn by itself to detect the elements it must know or recognize in order to achieve its mission.

With deep learning, the problem breaks down into a series of hierarchical correspondences - each mapping is described by a specific layer.

The entry (representing the variables that we could actually observe) is presented at the visible layer. Then, a series of so-called hidden layers extracts the more and more abstract characteristics. However, it should be noted that this process is not pre-defined, which means that we only specify what the layers select [36].

- For example: from pixels, the first hidden layer identifies the edges.
- From the edges, the second layer identifies the corners and outlines.
- From the corners and outlines, the third layer identifies parts of objects.
- Finally, from the object parts, the fourth layer identifies all the objects.

In addition, we have technological limitations. For example, we have a long way to go before we have a system that understands that you're sad because your cat is dead (but it looks like IBM Watson-based Cognitoys is moving in that direction). Therefore, the current focus is primarily on identifying photos, such as guess-

ing age from photos (based on the Microsoft Oxford API project). However, today, we remain technologically limited. Indeed, Google's neural network that identified cats had 16,000 nodes, while a human brain has about 100 billion neurons!

Temporal trends: In their recent study, PhD student Huan-Kai Peng and Professor Radu Marculescu, [37], from Carnegie Mellon University's Electrical and Computer Engineering Department, propose a new way of identifying the intrinsic dynamics of models' interactions at multiple time scales. Their approach consists in building a deep learning model that consists of several levels where each one captures patterns of a specific time scale. The newly proposed model can also be used to explain the different ways that short-term patterns relate to long-term patterns. For example, it becomes possible to describe how a long-term pattern on twitter can be sustainable and narrowed by a sequence of short-term patterns, including such characteristics as popularity, character, popular, contagious and interactivity.

4. CASE STUDY

The chosen area for the study of the influence of solar spots and global warming is the village EL AKARIT (9.645339, 34.1621899) located in the south east of Tunisia next to the city of GABES. This village was selected by the national electricity company STEG for the installation of a 100 MW power station.

Ground measurements of solar radiation show that production can exceed 1 kWh / m².

For this case study, we collected the solar irradiation data as well as the daily temperature values of minimum, maximum, wind speed, sky clarity index and sunspots values over a 33- year period of time (since 1985).

All data are obtained from practical ground measurements and from NASA satellites measurements as shown in Table 1.

We have opted to use KNIME© software to predict possible future production fluctuations as a result of climate change and solar activity. It is an opensource software used by more than 15,000 users in the world from different backgrounds (academia, research, small and large companies) in different sectors (banking, pharmacy, tourism, ...) has strong assets [38-40]:

- Its ease of use and its graphical interface make it accessible to the uninitiated in data mining.

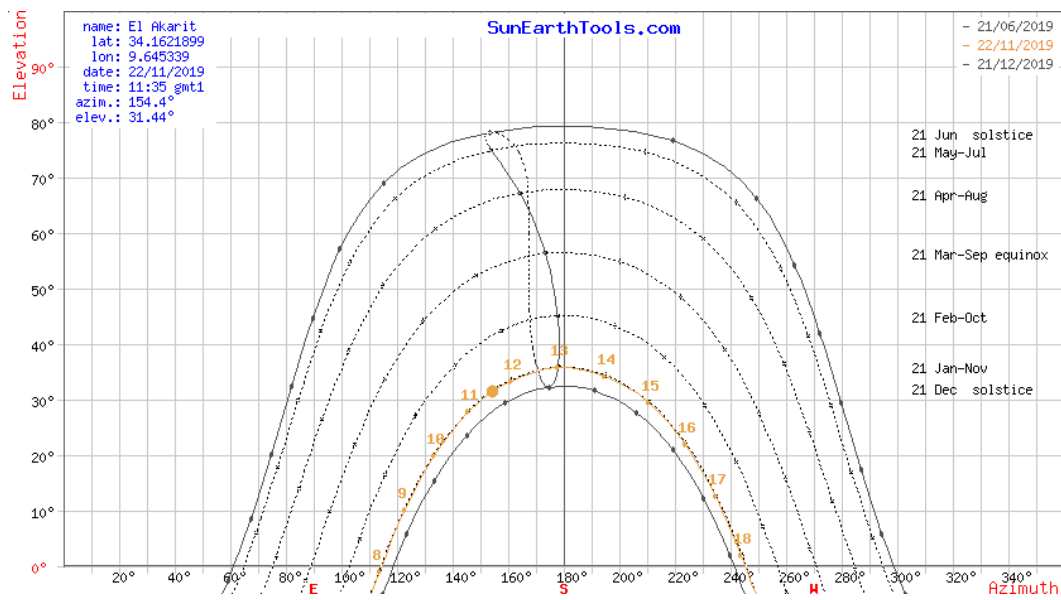


Figure 6: Sun trajectory throughout the year over the EL AKARIT region.

Table1: Data Inputs Algorithm

Years	GHI (kWh/m ²)	Max_Temp (°C)	Min_Temp (°C)	Ave_Temp (°C)	Wind Speed (m/s)	Clear Sky (%)	Partly Cloudy (%)	Mostly Cloudy (%)
1985	1785.46	34.18	4.69	19.54	4.13	31.25	61.93	6.82
1986	1778.5	32.42	6.82	19.56	4.14	30.97	62.50	6.53
1987	1700.5	34.46	4.65	19.69	4.09	23.53	68.63	7.84
..								
..								
2015	1950.51	34.68	5.33	19.92	3.98	60.66	36.64	2.70
2016	1922.98	34.67	7.59	21.04	4.16	52.92	43.38	3.69
2017	1943.06	35.44	5.6	19.64	4.24	60.42	36.86	2.72
2018	1898.71	36.23	7.94	20.18	4.07	52.60	43.12	4.28

- It can read many data formats.
- It contains many solutions to pre-process, analyze and visualize data and analysis results.
- The user community is very active and can help add new features to the software.

The model to be implemented in the KNIME© environment is described by the figure which details the used inputs and the expected outputs (Figure 7).

The practical implementation is detailed in the figure that shows the different blocks used as well as the ordering that constitutes the workflow (Figure 8).

The Lift curve applies to most statistical methods that calculate forecasts (expected classifications) for

binomial or multinomial responses. In STATISTICA, Lift curves can be calculated in different modules, including Classification / Regression Tree Templates (C & RT), CHAID Models, Generalized Linear / Non-Linear Models (Logit and Probit models for binomial responses), General Models Discriminant Analysis (GDA) (for binomial responses), etc. The Rapid Deployment Module of Predictive Models calculates simple or superimposed Lift curves (to compare several predictive models) based on the learning models and models deployed by PMML. This curve is often used in Data Mining projects as well as similar synthetic curves (Gain Curves), when the dependent or output variable studied is of a binomial nature.

A Matrix Confusion is a summary of the results of predictions on a classification problem. Correct and

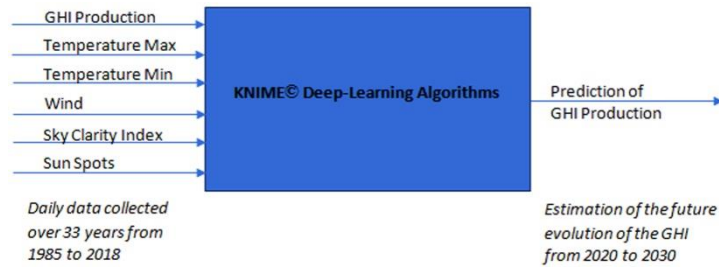


Figure 7: Inputs and Outputs model.

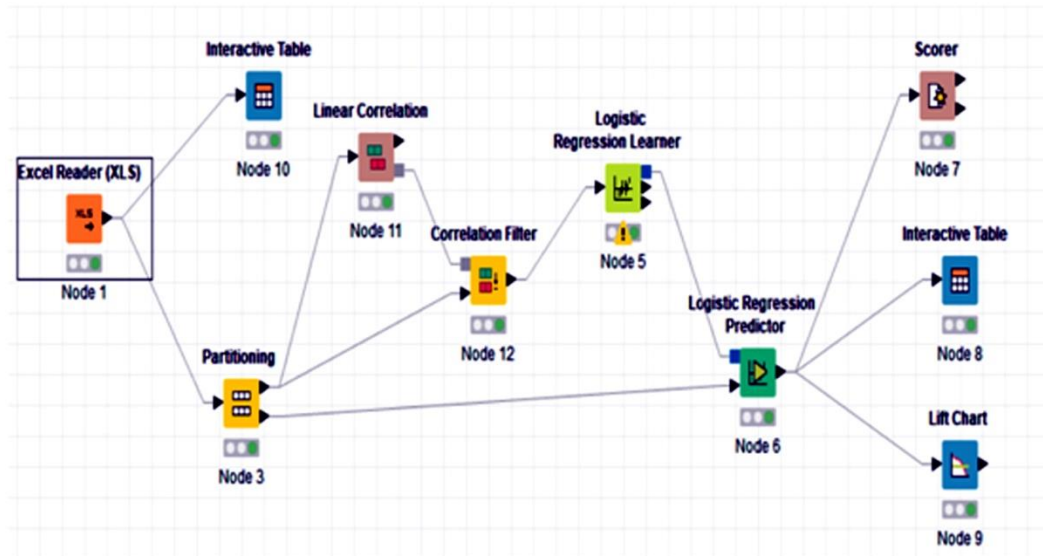


Figure 8: KNIME Workflow.

incorrect predictions are highlighted and divided by class. The results are thus compared with the actual values. This matrix helps to understand how the classification model is confused when making predictions. This allows not only knowing which errors are made, but especially the type of errors that have been made. Users can analyze them to determine which results indicate how mistakes are made.

To evaluate the future production of the site, and the possibility of a variation of production depending on global warming or solar activity we have to ensure in a first step a good training of the neurons used by tens of thousands of measurements collected from 1985 until 2018 (see Figure 7).

In a second step we combined the following possibilities for the years to come from 2020 to 2030:

- 1) Global warming of 0.5°C every three years with a decrease in solar activity;
- 2) A global warming of 0.5°C every three years with an increase in solar activity;

- 3) A drop-in temperature of 0.5°C every three years with a decrease in solar activity;
- 4) A drop-in temperature of 0.5°C every three years with a decrease in solar activity.

The obtained results must be verified using four of the most important verification criteria below to prove the accuracy and the reliability of the produced predictions:

1. the Accuracy indicator,
2. the Cohen's Kappa K indicator,
3. the area between the base line and the lift curve,
4. the estimated correlations between the different parameters in the Confusion Matrix.

In this study, the accuracy indicator is greater than 88%, a good percentage which gives the results a high degree of confidence (see Figures 11 and 12).

Let K be the Cohen's kappa coefficient used to measure the percentage of data values in the diagonal

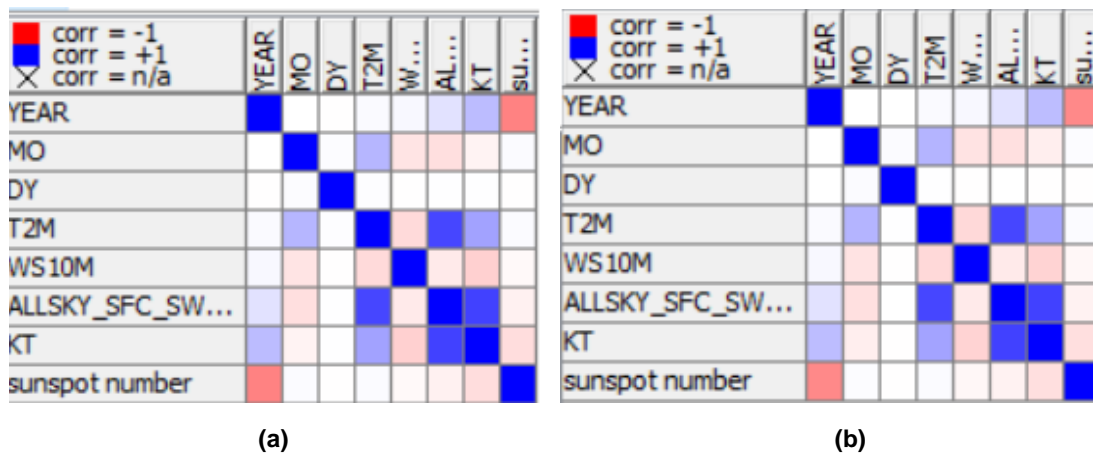


Figure 9: Confusion Matrices (a: case of decrease; b: case of increase).

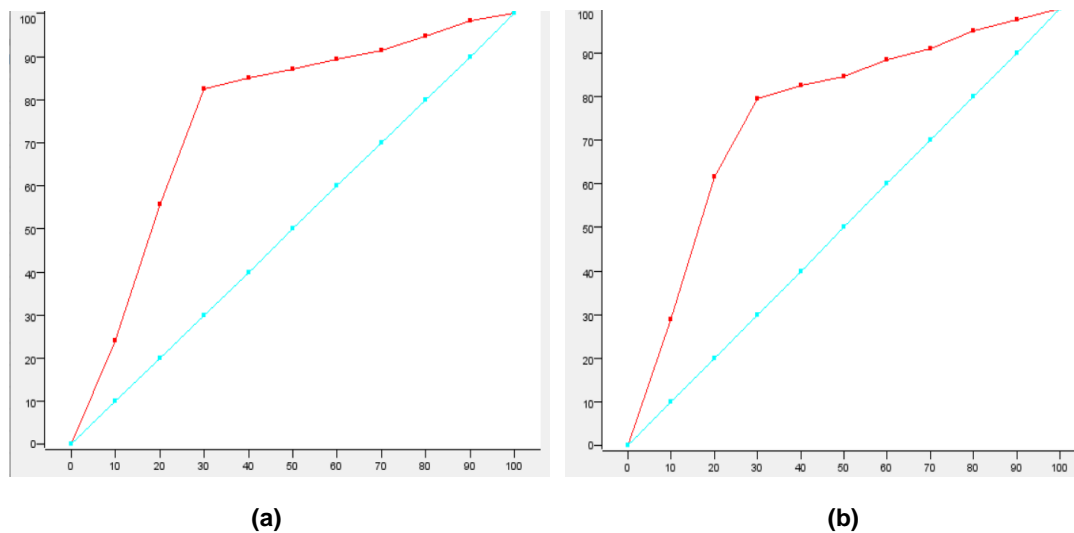


Figure 10: Lift Chart (a: case of decrease; b: case of increase).

of the confusion matrix table and then adjusts these values to make aleatory agreement occurring possible. K can be classified as follows:

- $K \in [0, 0,2]$ Poor agreement.
- $K \in [0,21, 0,4]$ Fair agreement.
- $K \in [0,41, 0,6]$ Moderate agreement.
- $K \in [0,61, 0,8]$ Good agreement.
- $K \in [0,81, 1]$ Very good agreement.

The correlation matrix (see Figure 9, a & b) is shown as a red-white-blue heatmap. Blue values show a high correlation, white values show correlation zero and red values show an inverse correlation between the two columns.

The cumulative gains chart (see Figure 10, a & b) is a visual aid used to measure model performances. So,

when the area between the lift curve and the baseline is great, the predictive model's performance is higher.

Table 2 shows that the effect of global warming is preponderant and that the production of a future power plant will increase by about 11%, (see cases d, e, f, g, h, and i) and that climatic disturbances will not have a significant effect on its production.

Table 2 below summarizes the results obtained at the output of the model:

According to the calculations, the following conclusions are deduced in a hierarchical order:

- The production of photovoltaic electric power will be increasing in the coming decade as in the last three decades even if there will be no increase in temperature or in solar activities. (see Table 2, case (e)). This conclusion seems logical because

Power \ Prediction	Min	Average	Max
Min	733	136	0
Average	110	2351	67
Max	0	85	902

Correct classified: **3986** Wrong Classified: **398**
Accuracy: **90.9 %** Error: **9.1 %**
Cohen's Kappa (K) **0.907**

Figure 11: Scoring in case of decrease of Sunspots

Power \ Prediction	Min	Average	Max
Min	598	213	0
Average	0	2391	150
Max	0	126	906

Correct classified: **3895** Wrong Classified: **489**
Accuracy: **88.8 %** Error: **11.2 %**
Cohen's Kappa (K) **0.846**

Figure 12: Scoring in case of increase of Sunspots.

Table 2: GHI Prediction (Main Results)

Solar Activities Temperature	↘	→	↗
↘	Case (a) 0% (-1.12 kWh/m ²)	Case (b) 2% (+29 kWh/m ²)	Case (c) 7% (+99 kWh/m ²)
→	Case (d) 7% (+99 kWh/m ²)	Case (e) 9% (+127 kWh/m ²)	Case (f) 11% (+155 kWh/m ²)
↗	Case (g) 8% (+114 kWh/m ²)	Case (h) 11% (+155 kWh/m ²)	Case (i) 12% (+170 kWh/m ²)

the neural network has memorized an increase of the production during the last three decades under the effect of the increase of the temperature which moves the MPPT towards higher voltages with a constant current, and thus towards more power.

- If a drop-in temperature will be observed, during the next decade, the production will not be affected in a significant way (case (a)). An increase in solar activity, in this case, will be able to improve production (case (b) and case (c)).

- An increase in temperature will produce, almost systematically, an increase in production and the effect of solar activity will not be very important (see cases (g), (h), and (i)).

According to the findings presented, the effect of global warming is more important than the effect of sunspots on the production of photovoltaic electrical energy. Our results are consistent with those provided by Georg Feulner and Stefan Rahmstorf of the Potsdam Institute for Climate Impact Research [41]. They claim that solar cycles will contribute to the

increase in global temperature only 0.26°C and that the main increase of 4°C that causes global warming is of human origin.

It should also be noted that the effect of the increase in production due to the increase in temperature is not linear and that, beyond certain values, a saturation effect is observed, and threatens to alter the panels. This effect is already a common issue among specialists.

CONCLUSION

The debate over the influence of solar activity on global warming and climatic variations is getting fiercer and more fueled. It has become more complicated and far from getting resolved. The mathematical models built, to date, have not yet been developed and require much more perfections. The use of Deep-Learning algorithms seems an efficient approach to compensate for the present lack of precision and clarity.

We have tried in this paper to use the new techniques of Machine-Learning to analyze the influences of the factors already mentioned on the climate and thus on the productivity of the photovoltaic and thermo-solar sites. The data used are daily measurements by NASA satellites of temperature, wind, power generation and sky conditions over the past 30 years.

Calculation results show that climate warming, and sunspots contribute to more electricity production. In the case of a decline in solar activity the effect of global warming is dominant and contributes to a climate change that will increase production, in the case studied in Tunisia for the next 7 years. It will, then, show a decline in the site's production (many more cloudy days) at the end of the next decade.

The addition of many more layers of neurons and other measured data, such as that of humidity, in the prediction algorithm will certainly lead to much more precision. However, this will require, certainly, many calculation tools and much more time.

SPECIAL THANKS

The authors would like to thank Mrs. Fatma Fattoumi for helping in editing this work.

REFERENCES

- [1] Derouich, W., Besbes, M., & Olivencia, J. D. (2014). Prefeasibility study of a solar power plant project and optimization of a meteorological station performance. *Journal of applied research and technology*, 12(1), 72-79. [https://doi.org/10.1016/S1665-6423\(14\)71607-4](https://doi.org/10.1016/S1665-6423(14)71607-4)
- [2] Othman, A. B., Belkilani, K., & Besbes, M. (2017). *Energy Reports*.
- [3] Kaouther, B., Othman, A., & Besbes, M. (2018, June). Estimation of Global and Direct Solar Radiation in Tunisia Based on Geostationary Satellite Imagery. In 2018 IEEE PES/IAS PowerAfrica (pp. 190-194). IEEE. <https://doi.org/10.1109/PowerAfrica.2018.8521155>
- [4] Belkilani, K., Othman, A. B., & Besbes, M. (2018) (a). Estimation and experimental evaluation of the shortfall of photovoltaic plants in Tunisia: case study of the use of titled surfaces. *Applied Physics A*, 124(2), 179. <https://doi.org/10.1007/s00339-018-1581-x>
- [5] Belkilani, Kaouther, Afef Ben Othman, and Mongi Besbes (2018) (b). "Assessment of global solar radiation to examine the best locations to install a PV system in Tunisia." *Applied Physics A* 124.2 (2018): 122. <https://doi.org/10.1007/s00339-018-1551-3>
- [6] Fathallah, M. A. B., Othman, A. B., & Besbes, M. (2018). Modeling a photovoltaic energy storage system based on super capacitor, simulation and evaluation of experimental performance. *Applied Physics A*, 124(2), 120. <https://doi.org/10.1007/s00339-018-1549-x>
- [7] Othman, A. B., Fathallah, M. A. B., & Besbes, M. (2019). Robust control of a photovoltaic pumping system with super-capacitor storage, P&O algorithm and pole placement technique. *Energy Systems*, 10(4), 1017-1041. <https://doi.org/10.1007/s12667-018-0295-7>
- [8] Zharkova, V. V., Arzner, K., Benz, A. O., Browning, P., Dauphin, C., Emslie, A. G., & Petrosian, V. (2011). Recent advances in understanding particle acceleration processes in solar flares. *Space science reviews*, 159(1-4), 357. <https://doi.org/10.1007/s11214-011-9803-y>
- [9] Zharkova, V. V., Aboudarham, J., Zharkov, S., Ipson, S. S., Benkhailil, A. K., & Fuller, N. (2005). Solar feature catalogues in EGSO. *Solar Physics*, 228(1-2), 361-375. <https://doi.org/10.1007/s11207-005-5623-0>
- [10] Shepherd, S. J., Zharkov, S. I., & Zharkova, V. V. (2014). Prediction of solar activity from solar background magnetic field variations in cycles 21-23. *The Astrophysical Journal*, 795(1), 46. <https://doi.org/10.1088/0004-637X/795/1/46>
- [11] Kopp, G., & Lean, J. L. (2011). A new, lower value of total solar irradiance: Evidence and climate significance. *Geophysical Research Letters*, 38(1). <https://doi.org/10.1029/2010GL045777>
- [12] Wang, Y., Ye, P., Zhou, G., Wang, S., Wang, S., Yan, Y., & Wang, J. (2005). The interplanetary responses to the great solar activities in late October 2003. *Solar Physics*, 226(2), 337-357. <https://doi.org/10.1007/s11207-005-6877-2>
- [13] Qahwaji, R., & Colak, T. (2006). Neural network-based prediction of solar activities. *CITSA2006: Orlando*, 4-7.
- [14] Beer, J., Tobias, S., & Weiss, N. (1998). An active Sun throughout the Maunder minimum. *Solar Physics*, 181(1), 237-249. <https://doi.org/10.1023/A:1005026001784>
- [15] Ammann, C. M., Joos, F., Schimel, D. S., Otto-Bliesner, B. L., & Tomas, R. A. (2007). Solar influence on climate during the past millennium: Results from transient simulations with the NCAR Climate System Model. *Proceedings of the National Academy of Sciences*, 104(10), 3713-3718. <https://doi.org/10.1073/pnas.0605064103>
- [16] DeLand, M. T., & Cebula, R. P. (2012). Solar UV variations during the decline of Cycle 23. *Journal of Atmospheric and Solar-Terrestrial Physics*, 77, 225-234. <https://doi.org/10.1016/j.jastp.2012.01.007>

- [17] White, W. B., Lean, J., Cayan, D. R., & Dettinger, M. D. (1997). Response of global upper ocean temperature to changing solar irradiance. *Journal of Geophysical Research: Oceans*, 102(C2), 3255-3266.
<https://doi.org/10.1029/96JC03549>
- [18] Krivova, N. A., & Solanki, S. K. (2008). Models of solar irradiance variations: Current status. *Journal of Astrophysics and Astronomy*, 29(1-2), 151-158.
<https://doi.org/10.1007/s12036-008-0018-x>
- [19] Unruh, T., Rempe, J., McGregor, D., Ugorowski, P., & Reichenberger, M. (2012). NEET Micro-Pocket Fission Detector--FY 2012 Status Report (No. INL/EXT-12-27274). Idaho National Laboratory (INL).
- [20] Lean, J. L., & DeLand, M. T. (2012). How does the Sun's spectrum vary?. *Journal of Climate*, 25(7), 2555-2560.
<https://doi.org/10.1175/JCLI-D-11-00571.1>
- [21] Cahalan, R. F., Wen, G., Harder, J. W., & Pilewskie, P. (2010). Temperature responses to spectral solar variability on decadal time scales. *Geophysical Research Letters*, 37(7).
<https://doi.org/10.1029/2009GL041898>
- [22] Lean, J., Rottman, G., Harder, J., & Kopp, G. (2005). SORCE contributions to new understanding of global change and solar variability. In *The Solar Radiation and Climate Experiment (SORCE)* (pp. 27-53). Springer, New York, NY.
https://doi.org/10.1007/0-387-37625-9_3
- [23] Haigh, I. D., Wijeratne, E. M. S., MacPherson, L. R., Pattiaratchi, C. B., Mason, M. S., Crompton, R. P., & George, S. (2014). Estimating present day extreme water level exceedance probabilities around the coastline of Australia: tides, extra-tropical storm surges and mean sea level. *Climate Dynamics*, 42(1-2), 121-138.
<https://doi.org/10.1007/s00382-012-1652-1>
- [24] Merkel, A. W., Harder, J. W., Marsh, D. R., Smith, A. K., Fontenla, J. M., & Woods, T. N. (2011). The impact of solar spectral irradiance variability on middle atmospheric ozone. *Geophysical Research Letters*, 38(13).
<https://doi.org/10.1029/2011GL047561>
- [25] Vigouroux, C., Blumenstock, T., Coffey, M., Errera, Q., García, O., Jones, N. B., ... & Mellqvist, J. (2015). Trends of ozone total columns and vertical distribution from FTIR observations at eight NDACC stations around the globe. *Atmospheric Chemistry and Physics*, 15(6), 2915-2933.
<https://doi.org/10.5194/acp-15-2915-2015>
- [26] LeCun, Y., Bengio, Y., & Hinton, G. (2015). Deep learning. *nature*, 521(7553), 436-444.
<https://doi.org/10.1038/nature14539>
- [27] Wang, J., Ma, Y., Zhang, L., Gao, R. X., & Wu, D. (2018). Deep learning for smart manufacturing: Methods and applications. *Journal of Manufacturing Systems*, 48, 144-156.
<https://doi.org/10.1016/j.jmsy.2018.01.003>
- [28] Schmidhuber, J. (2015). Deep learning in neural networks: An overview. *Neural networks*, 61, 85-117.
<https://doi.org/10.1016/j.neunet.2014.09.003>
- [29] Nielsen, M. A. (2015). *Neural networks and deep learning* (Vol. 25). San Francisco, CA, USA: Determination press.
- [30] Ngiam, J., Khosla, A., Kim, M., Nam, J., Lee, H., & Ng, A. Y. (2011). Multimodal deep learning. In *Proceedings of the 28th international conference on machine learning (ICML-11)* (pp. 689-696).
- [31] Paugam-Moisy, H. (2006). *Spiking neuron networks a survey* (No. REP_WORK). IDIAP.
- [32] Bertsekas, D. P. (2011). Incremental gradient, subgradient, and proximal methods for convex optimization: A survey. *Optimization for Machine Learning*, 2010(1-38), 3.
- [33] Griesse, R., & Walther, A. (2004). Evaluating gradients in optimal control: continuous adjoints versus automatic differentiation. *Journal of optimization theory and applications*, 122(1), 63-86.
<https://doi.org/10.1023/B:JOTA.0000041731.71309.f1>
- [34] Wu, A. G., Dong, R. Q., & Fu, F. Z. (2015). Weighted stochastic gradient identification algorithms for ARX models. *IFAC-PapersOnLine*, 48(28), 1076-1081.
<https://doi.org/10.1016/j.ifacol.2015.12.274>
- [35] Hofmann, T., Lucchi, A., Lacoste-Julien, S., & McWilliams, B. (2015). Variance reduced stochastic gradient descent with neighbors. In *Advances in Neural Information Processing Systems* (pp. 2305-2313).
- [36] Mesejo, P., Ibáñez, O., Fernández-Blanco, E., Cedrón, F., Pazos, A., & Porto-Pazos, A. B. (2015). Artificial neuron-glia networks learning approach based on cooperative coevolution. *International journal of neural systems*, 25(04), 1550012.
<https://doi.org/10.1142/S0129065715500124>
- [37] Peng, H. K., Lee, H. C., Pan, J. Y., & Marculescu, R. (2016). Data-Driven Engineering of Social Dynamics: Pattern Matching and Profit Maximization. *PloS one*, 11(1), e0146490.
<https://doi.org/10.1371/journal.pone.0146490>
- [38] O'Hagan, S., & Kell, D. B. (2015). Software review: the KNIME workflow environment and its applications in Genetic Programming and machine learning. *Genetic Programming and Evolvable Machines*, 16(3), 387-391.
<https://doi.org/10.1007/s10710-015-9247-3>
- [39] Jagla, B., Wiswedel, B., & Coppée, J. Y. (2011). Extending KNIME for next-generation sequencing data analysis. *Bioinformatics*, 27(20), 2907-2909.
<https://doi.org/10.1093/bioinformatics/btr478>
- [40] Berthold, M. R., Cebon, N., Dill, F., Gabriel, T. R., Kötter, T., Meinel, T., & Wiswedel, B. (2009). KNIME-the Konstanz information miner: version 2.0 and beyond. *AcM SIGKDD explorations Newsletter*, 11(1), 26-31.
<https://doi.org/10.1145/1656274.1656280>
- [41] Feulner, G., Rahmstorf, S., Levermann, A., & Volkwardt, S. (2013). On the origin of the surface air temperature difference between the hemispheres in Earth's present-day climate. *Journal of climate*, 26(18), 7136-7150.
<https://doi.org/10.1175/JCLI-D-12-00636.1>

Received on 2-12-2020

Accepted on 27-12-2020

Published on 31-12-2020

DOI: <http://dx.doi.org/10.31875/2410-2199.2020.07.8>© 2020 Othman *et al.*; Zeal Press.

This is an open access article licensed under the terms of the Creative Commons Attribution Non-Commercial License (<http://creativecommons.org/licenses/by-nc/3.0/>) which permits unrestricted, non-commercial use, distribution and reproduction in any medium, provided the work is properly cited.